Piecewise coherent mode processing of acoustic data recorded on two horizontally separated vertical line arrays

Ilya A. Udovydchenkov
Applied Ocean Physics and Engineering Department, Woods Hole Oceanographic Institution, Woods Hole, Massachusetts 02543
ilya@whoi.edu

Michael G. Brown
Rosenstiel School of Marine and Atmospheric Science, University of Miami, Miami, Florida 33149
mbrown@rsmas.miami.edu

Timothy F. Duda
Applied Ocean Physics and Engineering Department, Woods Hole Oceanographic Institution, Woods Hole, Massachusetts 02543
tduda@whoi.edu

Abstract: Motivated by measurements made in the 2004 Long-Range Ocean Acoustic Propagation Experiment (LOAPEX), the problem of mode processing transient acoustic signals collected on two nearby vertical line arrays is considered. The first three moments (centroid, variance, and skewness) of broadband distributions of acoustic energy with fixed mode number (referred to as modal group arrivals) are estimated. It is shown that despite the absence of signal coherence between the two arrays and poor high mode number energy resolution, the centroid and variance of these distributions can be estimated with tolerable errors using piecewise coherent mode processing as described in this paper.

PACS numbers: 43.30.Bp, 43.60.Ac, 43.60.Fg [JFL]
Date Received: January 31, 2012 **Date Accepted:** May 10, 2012

1. Introduction

The work reported here was motivated by measurements collected during the 2004 Long-Range Ocean Acoustic Propagation Experiment (LOAPEX) (see Mercer *et al.*, 2005; Mercer *et al.*, 2009) that was conducted in the eastern North Pacific Ocean. In that experiment, broadband transmissions in the 50–100 Hz band from a ship-suspended compact source were received at several ranges on two adjacent (separated by about 5 km) vertical line arrays (VLAs) of hydrophones. One of the two VLAs, the shallow VLA, or SVLA, was centered approximately on the sound channel axis and resolved the lowest 10 or so modes. The second VLA was deeper and is referred to as the deep VLA, or DVLA. The difference in propagation range between the SVLA and the DVLA was sufficiently short that there was negligible redistribution of modal energy between the two measurement locations, but sufficiently large that phase coherence between measurements made at the two locations was lost. The motivation for the work reported here was a desire to estimate the three lowest moments (centroid, variance, and skewness) of modal group arrivals, i.e., broadband distributions of acoustic energy corresponding to fixed mode number. In this letter, it is shown that a procedure, known as "piecewise coherent mode processing," which is described, can be used to estimate these quantities using LOAPEX-like data. The utility of piecewise coherent mode processing for other purposes is not investigated here.

In this paper, synthetic data, constructed using the RAM (Collins and Westwood, 1991; Collins, 1993) acoustic propagation model, is analyzed. The geometry and environment used in the simulations closely resemble LOAPEX conditions. In this environment, there are approximately 80 non-surface-reflecting and non-bottom-reflecting propagating modes at 75 Hz. Errors associated with the use of piecewise coherent processing estimates of modal group arrival statistics are assessed at four different transmission ranges used in LOAPEX. It is shown that these errors are generally tolerable for performing tomographic inverses and testing theoretical predictions of modal group time spreads. In Sec. 2, the piecewise coherent mode processing algorithm is described. Results are presented in Sec. 3, and conclusions are given in Sec. 4.

2. Piecewise coherent mode processing

It is useful to describe the LOAPEX measurements in more detail before explaining the piecewise coherent mode processing algorithm. The horizontal separation between the SVLA and the DVLA was approximately 5.4 km; the range separation between the SVLA and the DVLA along the propagation paths was 5.3 km. Neighboring hydrophones on both the SVLA and the DVLA were separated by 35 m. The SVLA consisted of 40 hydrophones covering depths between 350 and 1750 m. The DVLA consisted of two 20 hydrophone segments covering depths between 2150 and 2850 m, and between 3570 and 4270 m. The transmission ranges used in the simulations are the LOAPEX transmission ranges from stations T50, T250, T500, and T1000. These ranges are 44.7, 284.7, 484.7, and 984.7 km from the source to the SVLA, and, in each case, 5.3 km greater to the DVLA. In the simulations shown, the acoustic source depth was 800 m; broadband pulses with 75 Hz center frequency were simulated. The source spectrum was assumed to have the shape of a Hanning window with zeros at 56.25 and 93.75 Hz; the corresponding bandwidth (full width at half amplitude) was 18.75 Hz. In the simulations, it is assumed that the source and all receivers are stationary, that both receiving arrays are vertical, and that the depth separation between hydrophones is exactly 35 m. It is also assumed in the simulations that the positions of the source and all hydrophones are known and that there are no timing errors.

Figures 1(a)–1(d) show examples of simulated acoustic wave fields recorded by the SVLA and the DVLA for T50, T250, T500, and T1000 transmissions, respectively. The environment used in these simulations consisted of a range-independent sound speed profile on which a range-dependent perturbation due to internal waves (Colosi and Brown, 1998) was superimposed. The LOAPEX environment can be accurately described by a model of this type for ranges up to 1000 km. The background profile is a range-averaged profile over 1000 km between the DVLA and the T1000 station derived from a set of profiles provided by Lora Van Uffelen (personal communication). The topography was flat with a constant depth of 5000 m. A homogeneous bottom with compressional velocity $c_p = 1.6$ km/s, density $\rho = 1350$ kg/m^3, and

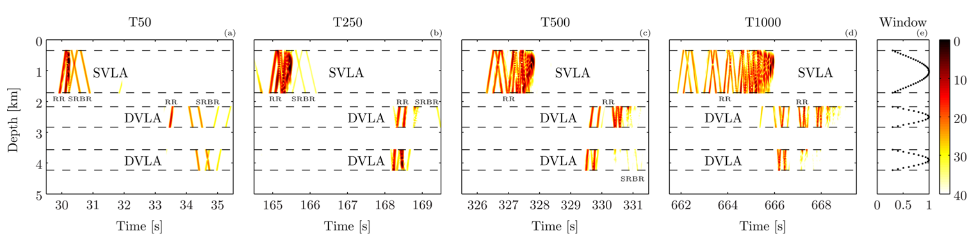

Fig. 1. (Color online) (a)–(d) Simulated acoustic wave fields for transmission from stations T50, T250, T500, and T1000 recorded by the SVLA and the DVLA. Refracted-refracted (or surface-reflected bottom-refracted) (RR) and surface-reflected bottom-reflected (SRBR) arrivals are labeled on each panel. The color bar shows relative wave field intensities in dB. (e) Windowing function applied to the simulated wave fields in the mode filtering process.

attenuation $\alpha = 10$ dB/wavelength was used. To investigate the influence of bottom-reflected signals on processing results for transmissions from T50, additional simulations were performed with a weakly reflecting bottom ($c_p = 1.54242$ km/s, $\rho = 1000$ kg/m^3, and $\alpha = 0.05$ dB/wavelength). In Fig. 1, intensities were normalized to the peak intensity value at each range. These wave fields (or their frequency domain counterparts) are the starting point for mode filtering.

Now the piecewise-coherent mode processing algorithm is described. At each frequency within the excited band, mode filtering was performed separately on the simulated SVLA and the DVLA wave fields. Then, collecting energy at fixed mode number m and Fourier transforming back to the time domain gives two sets of modal group arrivals. Because of the difference in range to the SVLA and the DVLA, the time dependence of each distribution at each m was converted to dependence on group slowness, $S_g = t/r$. The two sets (SVLA and DVLA) of energy distributions at each m were then incoherently added. We refer to the process just described as piecewise coherent mode processing. The result is an approximation to the energy distribution (vs S_g at each m) that would have resulted had the SVLA and the DVLA been co-located. Mode filtering was performed using the direct projection method, which is both stable and efficient. Another very important property of the direct projection filter in the present context is that it conserves energy. At each frequency, the total energy in the estimated modal amplitudes is identical to the total energy in the corresponding VLA measurements–as it should (Udovydchenkov *et al.*, 2010). This property also carries over to the incoherent sums of energy in the piecewise coherently processed fields; the energy in those fields is identical to the sum of the energies in the SVLA and the DVLA measurements. To suppress modal cross-talk, the VLA measurements were windowed as indicated in Fig. 1. It should be noted that mode filtering is closely related to estimation of Fourier spectra inasmuch as in both cases one attempts to expand measurements in a set of basis functions that are the eigenvectors of a Sturm–-Liouville equation. With this connection in mind, the utility of using windows when mode filtering should come as no surprise. Finally, because the quantity of interest in this study is the mean distribution of energy vs S_g at each m, 100 realizations of the internal-wave-induced perturbation field were generated. Acoustic pulses were propagated in each environment. The centroid, variance, and skewness of the mode-processed arrival distribution at each m were computed; these estimates were subsequently averaged. (The number of realizations in the ensemble was limited by the computational burden; simulating actual LOAPEX conditions would require many more realizations.)

To compute modal arrival statistics, the acoustic wave fields were "time-gated" to discard bottom reflected signals (mostly at T50) and ensure that no wrap-around occurs at longer ranges. A reference sound speed of 1.478 km/s (approximately the minimum value in the background profile) was chosen. The corresponding reference arrival time is $t_0 = r/c_0$, where r is the transmission range. Time windows around t_0 were chosen to be [−0.75; 0.25], [−1.25; 0.25], [−2.00; 0.25], and [−5.00; 0.25] s for T50, T250, T500, and T1000, respectively. Data outside of these windows were discarded. The resulting wave fields were visually inspected to ensure that no signal had been discarded. The numerical noise floor was assumed to be 40 dB below the peak value in each of the mode-processed wave fields, and all signals below this threshold were discarded. Before converting estimated standard deviations into modal group time spreads, one has to take into account the fact that the noise floor placed at 40 dB threshold below the peak value results in a variable signal-to-noise ratio (SNR) for individual modal arrivals. An idealized Gaussian pulse was constructed, and standard deviations of this pulse as a function of truncation level were computed to mimic variable SNR. The data-simulated standard deviations were multiplied by the ratio of standard deviation of a Gaussian pulse with infinite SNR to the standard deviation of a Gaussian pulse with a given finite SNR. This procedure does not recover the structure of a pulse below the noise floor, but it eliminates the problem of time spreads being largely underestimated for small SNR. Finally, to facilitate the comparison of modal group time spread estimates with theoretical predictions (Udovydchenkov and Brown, 2008), the resulting spreads were multiplied by $\sqrt{2\pi}$. Skewnesses were computed as third moments of modal pulse amplitudes normalized by the standard deviation cubed.

3. Results

The results of the simulations performed are summarized in Figs. 2–4. Modal arrival statistics were computed in three different ways, using (1) a full dense array covering the entire water column with 5 m spacing between hydrophones, (2) SVLA data only, and (3) piecewise coherently processed SVLA and DVLA data. Estimated mean slownesses, time spreads, and skewnesses are shown in the upper rows of these figures, and estimated errors are shown in the bottom rows for four different transmission ranges. The figures show that errors decrease as the propagation range increases. It is also clear from the figures that the errors are significantly reduced if the data from both arrays are used rather than the SVLA data alone. The statistics for mode numbers greater than 55 cannot be estimated at T250 using the SVLA data only because all of the SVLA-based energy attributed to those modes is below the noise level threshold.

Figure 2 shows that the errors in group slowness estimates at T250, T500, and T1000 are an order of magnitude smaller than those estimated at T50. While at T50 there is no clear benefit from combining the data from the two arrays, a significant improvement is clearly seen in simulations made at T250, T500, and T1000. At T1000, the relative error does not exceed 0.01% for all modes. However, one needs to quantify how significant these errors are for practical applications. In a tomographic inversion, the errors in estimated travel time (or group slowness) result in environmental uncertainty. This uncertainty in the sound speed is the same order of magnitude as the relative error in group slownesses. This means that 0.01% error in group slowness estimates will result in about 15 cm/s error in the inverted sound speed profile, which is much smaller than the variations at fixed depth along the propagation path from T1000 to the DVLA (in the upper 1 km), as shown in Fig. 2(b). In other words, to

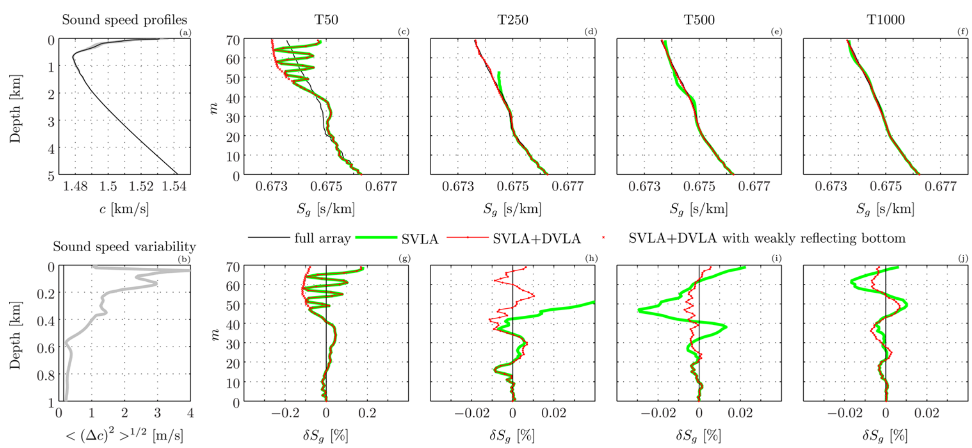

FIG. 2. (Color online) (a) Background sound speed profile used for numerical simulations is shown by the black curve. Gray curves show 395 profiles between T1000 and DVLA. (b) One standard deviation of the sound speed variations as a function of depth is shown by the thick gray curve. The black vertical line shows the estimated tomographic inversion error of 15 cm/s. (c)–(j) Estimates of group slowness (top row) and relative errors in group slowness (bottom row) as a function of mode number for three different array geometries. (1) Dense array covering the entire water column with 5 m spacing between hydrophones, (2) SVLA only data (thick curves), (3) piecewise coherently processed SVLA and DVLA data (dash-dot curves), and (4) piecewise coherently processed SVLA and DVLA data at T50 with a weakly reflecting bottom (×).

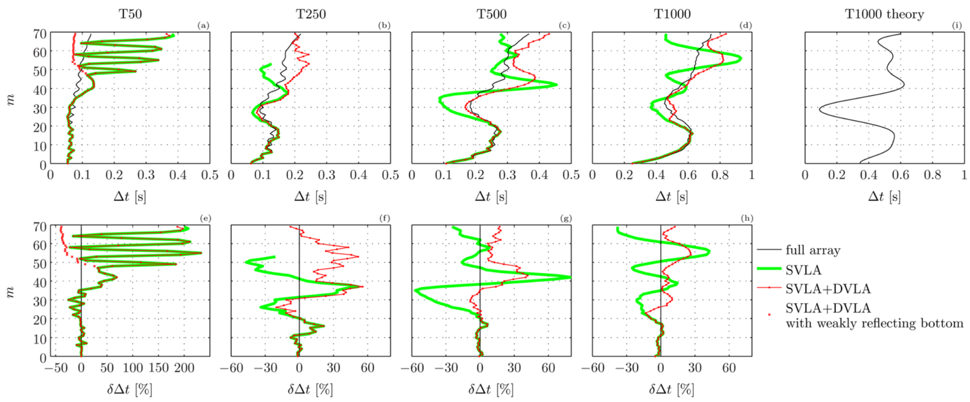

FIG. 3. (Color online) (a)–(h) Estimates of modal group time spreads (top row) and relative errors in modal group time spreads (bottom row) as a function of mode number for the same three array geometries that are described in the caption of Fig. 2. (i) Theoretical estimate of modal group time spreads at T1000.

perform tomographic inversions, T250, T500, and T1000 errors in mean group slowness estimates associated with piecewise coherent mode processing are negligibly small.

Modal group time spread estimates are shown in Fig. 3. As is the case for mean group slowness estimates, errors are much larger for the T50 simulations than for the T250, T500, and T1000 simulations with a reflective bottom. In the latter case, the piecewise-coherent time spread estimates shown differ at most from the full array time spread estimates by 27% (for T250 and T500 simulations relative errors are slightly larger, 56% and 42%, respectively). The errors at T50 for modes with $m \geq 48$ are significantly reduced (do not exceed 40%) with bottom reflections suppressed. Thus bottom-reflected arrivals may significantly contaminate processing results. Again one needs to quantify how much error is tolerable for a particular application. Theoretical estimates (Udovydchenkov and Brown, 2008) at T1000 are shown in Fig. 3(i). For the purpose of comparing simulated measurements with theory, the piecewise coherently processed measurements do not differ significantly from the processed full array

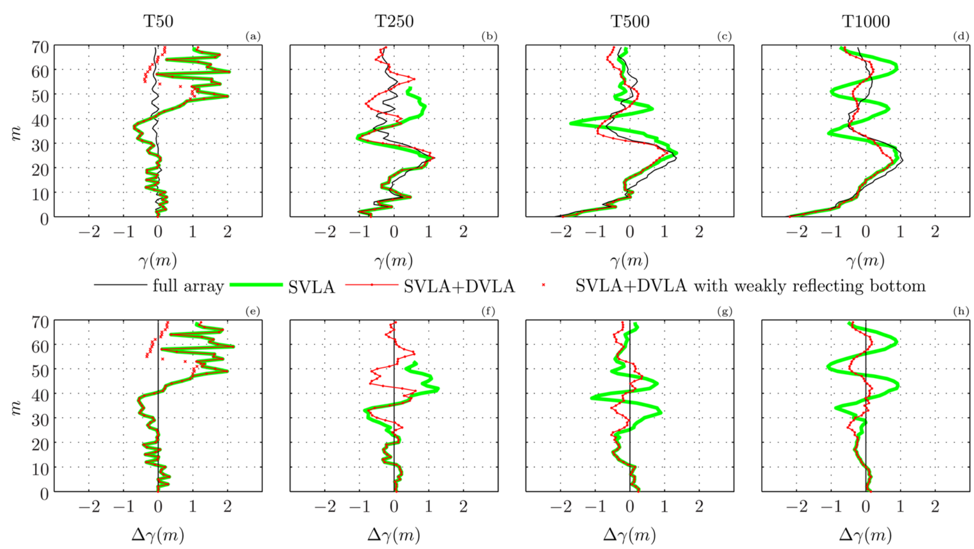

FIG. 4. (Color online) Estimates of skewness (top row) and absolute errors in skewness (bottom row) as a function of mode number for the same three array geometries that are described in the caption of Fig. 2.

measurements; the principal features of the piecewise coherent and full array Δt vs m curves are essentially the same. It should be emphasized that the issue that is investigated in this letter is how well the piecewise coherent and full-array based estimates of ΔS_g vs m agree with each other, and not how well those estimates agree with theoretical predictions; the utility of the theoretical estimate is that it provides a measure of what constitutes large and small errors.

Finally, Fig. 4 shows results of a similar analysis performed for estimated skewnesses. In this case, it is not practical to consider relative errors because the skewness typically has values close to zero. Instead, absolute errors are plotted in the bottom row of Fig. 4. These results suggest that the agreement is mostly qualitative. At T50, the distortions of modal arrivals caused by dispersion and scattering are very small. Because the emitted pulse is initially symmetric in time, the skewnesses of all modal arrivals are close to zero. For T250, T500, and T1000 transmissions, skewnesses estimated using the full array and piecewise coherent processing are in good qualitative agreement for mode numbers up to approximately 30, 40, and 45, respectively. For higher mode numbers the absolute error is seen to be the same order of magnitude as the value of the skewness itself.

4. Conclusions

Motivated by measurements made in the LOAPEX experiment, an attempt was made to mode process simulated SVLA and DVLA measurements using the piecewise coherent mode processing method described here. The objective was to determine whether this processing scheme can be used to estimate the lowest moments of modal group arrival distributions under LOAPEX-like conditions. It was determined that at ranges of 250, 500, and 1000 km, but not 50 km, errors in estimates of the first and second moments of these distributions are sufficiently small that the first moments allow tomographic inversions to be performed, and the second moments provide a meaningful test of theoretical predictions of modal group time spreads. Third moment estimates were also in good qualitative agreement with full-array-based estimates; in the absence of a theoretical estimate of this quantity or some other metric of error magnitudes, it is difficult to make a stronger statement. It was concluded that bottom-reflected arrivals significantly contaminate the statistics of modal group time spreads for modes with $m \geq 48$ at 50 km range, and these errors are smaller when bottom reflections are suppressed. It was also concluded that the piecewise coherent processing method used in this paper is more useful at longer ranges. The likely explanation for this behavior is that the loss of phase information associated with piecewise coherent processing is more harmful at short range than at long range. At longer ranges and at higher frequencies, phases tend to be more random due to scattering effects along the propagation path. As a result, the introduction of phase errors in processing algorithms is less harmful at long range and at higher frequencies that at shorter ranges and lower frequencies where phases are less random. With this in mind, it is expected that piecewise coherent processing works better at longer ranges, higher frequencies, and in environments with stronger fluctuations.

Acknowledgments

This work was supported by the Office of Naval Research, Code 322, Grant Nos. N00014-06-1-0245, N00014-08-1-0195, and N00014-11-1-0194.

References and links

Collins, M. (**1993**). "A split-step Padé solution for the parabolic equation method," J. Acoust. Soc. Am. **93**, 1736–1742.

Collins, M. D., and Westwood, E. K. (**1991**). "A higher-order energy-conserving parabolic equation for range-dependent ocean depth, sound speed and density," J. Acoust. Soc. Am. **89**, 1068–1075.

Colosi, J. A., and Brown, M. G. (**1998**). "Efficient numerical simulation of stochastic internal-wave-induced sound speed perturbation fields," J. Acoust. Soc. Am. **103**, 2232–2235.

Mercer, J. A., Andrew, R. K., Howe, B. M., and Colosi, J. A. (**2005**). "Cruise report: Long-range ocean acoustic propagation experiment (LOAPEX)," Technical Report APL-UW TR0501 (Applied Physics Laboratory, University of Washington, Seattle, WA).
Mercer, J. A., Colosi, J. A., Howe, B. M., Dzieciuch, M. A., Stephen, R., and Worcester, P. F. (**2009**). "LOAPEX: The Long-Range Ocean Acoustic Propagation Experiment," IEEE J. Ocean. Eng. **34**, 1–11.
Udovydchenkov, I. A., and Brown, M. G. (**2008**). "Modal group time spreads in weakly range-dependent deep ocean environments," J. Acoust. Soc. Am. **123**, 41–50.
Udovydchenkov, I. A., Rypina, I. I., and Brown, M. G. (**2010**). "Mode filters and energy conservation," J. Acoust. Soc. Am. **127**, EL185–EL191.